NASA TECHNICAL MEMORANDUM

NASA TM X-62,027

NASA TM X-62,027

MARTIAN DOUBLET CRATERS

Verne R. Oberbeck and Michio Aoyagi

Ames Research Center
Moffett Field, Calif. 94035

July 1971

MARTIAN DOUBLET CRATERS

VERNE R. OBERBECK AND MICHIO AOYAGI

Ames Research Center, NASA

Moffett Field, California 94035

ABSTRACT

A large number of Mars craters exist that are nearly tangential to other craters. They occur in clusters or as isolated crater doublets. Results of probability calculations and a Monte Carlo cratering simulation model show conclusively that many of the Mars craters could not have resulted from random single body impact. However, clusters and doublets could be caused by meteoroid breakup resulting from stresses induced in the meteoroid by the gravitational field of Mars. Calculations are provided that show the required relationships between mass, entry angle, impact velocity, and tensile strength of the meteoroid, and the separation distance between the centers of the resulting craters relative to crater sizes. It is concluded that under certain conditions, doublets should be produced on Mars as a direct result of breakup of an impacting meteoroid. The impact process can yield nonrandom crater distributions that should be observed in different degrees of development on different planetary surfaces. Thus, distributions of large craters on different planetary bodies cannot be compared directly for interpretations of the geologic history of one planetary surface relative to another.

INTRODUCTION

Examination of Mariner 6 and 7 photographs has revealed a large number of craters on Mars that are tangential or nearly tangential to one another. The hypothesis that all craters were formed by random single-body impact was tested through examination of the results of a series of Monte Carlo computer simulations of random impact cratering and through an independent probability computation. Both the Monte Carlo simulation and the probability calculation show that it is probable that most of the Mars doublets have not been produced by a random process.

The only endogenous mechanism for doublet crater production that seems possible is the formation of calderas. However, terrestrial calderas are not as large as most of the Martian craters, and terrestrial volcano-tectonic depressions, representative of the largest calderas, are markedly noncircular. In the past, it usually was assumed that impact of cosmic debris on any planetary body should produce random crater patterns. However, recent studies of probable impact craters on Earth contradict this assumption. The Clearwater Lakes craters (Figure 1) in Canada, consist of one 32-km diameter crater which is almost perfectly tangential to a 22.5-km crater. Both craters are generally accepted as impact craters because basement rocks have features characteristic of those produced by high-pressure shock waves [Dence, 1965]. There appears to be little doubt that two meteoroids impacted simultaneously to produce the Clearwater Lakes craters. Only the mechanism leading to the presence of two separate impacting bodies above the impact site at the same time is in question. Fig. 1

Sekiguchi [1970] has recently proposed a theory, which as qualified and supplemented in this study, accounts for the splitting of an impacting meteoroid

as it approaches a planet or satellite. He concludes that gravitational forces acting on an impacting meteoroid may cause internal stresses that exceed the meteoroid's tensile strength, causing it to split into bodies of approximately equal size. This type of calculation can be compared to the well-known calculation of the Roche limit, the critical altitude for which the difference in gravitational attraction between the planet and a very large body approaching the planet is greater than the mutual attraction of the mass elements of the impacting body. The Roche limit calculation assumes that the bodies are cohesionless. It is clear that bodies producing the Mars craters, with diameters between meters and kilometers must have had a finite tensile strength.

The plausibility of tidal splitting and separation as a means of Mars doublet formation will be examined in terms of the required relationships between mass, tensile strength, entry velocity, and entry angle of the meteoroid, and the crater separation distances and diameters.

OBSERVATIONS

Mariner 6 and 7 photographs of cratered terrain in Meridiani Sinus, Deucaleonus Regio, and Hellespontus (Figure 2) were studied. Nonrandom effects were first noticed for four crater pairs, labeled 1 through 4 in Figure 3. The ordering of crater arrangement exhibited by these crater pairs was particularly striking because each crater is nearly perfectly tangential to, and of about the same apparent age as its neighbor, and craters of a given doublet are nearly equal in size. It seems highly unlikely that doublets with these characteristics could

Fig. 2

Fig. 3

have been formed by random impact of single bodies. Other isolated crater pairs are labeled 5 through 8 in Figure 3; crater doublets occurring in groups of more than two craters are shown in crater clusters labeled 9 through 13. If a doublet is defined as any two craters that overlap or are separated by no more than 12.5 km, it can be shown that there are 461 crater doublets present in photographs 6N17, -19, -21, -23, and 7N25; this is a very large number when it is considered that there are only 906 craters larger than 4 km in the area photographed.

Figures 4a and b show the size distribution of these craters and the distribution of overlap or separation for the 461 doublets. The ratio of the radius of the largest crater (R_{max}) to the radius of the smallest crater (R_{min}) of each Martian doublet has been determined and the number of Martian doublets as a function of R_{max}/R_{min} is shown in Figure 4c. Inspection of the Figure 4c and the photographs suggests an ordering of crater size for members of doublets that is unlikely if all the craters were produced by bodies having equal probability of impacting at any position on the surface of Mars. Members of doublets are often of similar size. The distribution of Figure 4c is later compared to similar distributions resulting from the Monte Carlo simulations. Fig. 4

MONTE CARLO SIMULATION MODEL OF MARTIAN CRATERING

The Monte Carlo model of Martian cratering involves the drawing, at random, of craters from the crater size frequency distribution of Figure 4a. Next, random coordinates are selected for each of the craters drawn from the distribution and these are used to determine whether a given crater is close enough to any other crater to form a doublet. Random numbers between 0 and 1 are produced by one of two pseudorandom number generators of a class known and described as multiplicative

congruent generators [Fassone, et al., 1968]. That is, the generators are defined by the recurrence relationships, $U_{i+1} = aU_i \bmod(2^{31})$ where the parameter a is defined as 5^9 [Marsaglia, 1968] and $(2^{16} + 3)$ (IBM 360 Scientific Subroutine Package) for the respective generators.

The selection of a given crater diameter from the size frequency distribution of Martian craters (Figure 4a) is accomplished by first drawing a uniform random number u. Then, inverse interpolation is performed until the crater diameter D is obtained at which the cumulative distribution of diameter lengths equal u. Crater diameters given in Figure 4a are actually slightly larger than true values because the photographs show slightly oblique views of the surface. However, the effect of overestimates of crater diameter is to produce maximum possible numbers of doublets in the cratering simulation. An independent calculation shows that this leads to overestimates of the number of doublets of less than 10 percent. Selection of random x,y coordinates for the crater is accomplished by generating two numbers between 0 and 1 and multiplying each by the square root of the area being cratered (1843.1 km). The roles of the two generators used for selection of diameters and coordinates are also reversed in the cratering model for checks on randomness.

The next step in the Monte Carlo simulation is to determine whether a given crater, drawn at random, and assigned random coordinates, forms a doublet with any of the previous craters. This occurs when any of the following inequalities is satisfied:

$$r_i + r_j - \Delta \leq \left[(x_i - x_j)^2 + (y_i - y_j)^2\right]^{1/2} \leq r_i + r_j + \Delta \quad i < j, \; j = 1 \ldots 906 \tag{1}$$

where r_i is the radius of the ith crater drawn and r_j is the radius of the jth crater, x_i and x_j are the random x coordinates of the ith crater and jth crater, and y_i and y_j are the random y coordinates of the ith crater and the jth crater; Δ is the overlap or separation allowed for the particular crater pair in question. This value is selected at random from the distribution of Δ for doublets observed on Mars in the same way as crater radius is selected. Each Monte Carlo cratering simulation involves $j - 1$ separate solutions of inequality (1) for each of the craters j. All doublets resulting from satisfactory solutions of these inequalities were totaled and recorded by crater number, radius, and coordinates of each member of the doublet. For all doublets, the maximum radius was divided by the minimum radius and doublets were grouped according to classes of R_{max}/R_{min}. The use of all 906 craters in the computation completes one simulation of Martian cratering.

Simulation of the 906 cratering events was repeated 150 times; the resulting variation in numbers of doublets was as expected if the Martian cratering were random and accomplished 150 times. The statistical characteristics of this distribution and the number of doublets by R_{max}/R_{min} classes were computed. They were then compared to the corresponding Martian data to determine whether the cratering is nonrandom and to locate the classes of Martian doublets that contain most of the doublets produced by the nonrandom process.

RESULTS OF MONTE CARLO CRATERING MODEL

The results of the Monte Carlo simulation are shown in Figures 5a and b. Fig. 5
Figure 5a shows the distribution of the number of doublets that resulted. The

average number of doublets that occurred was 137 and two standard deviations were 26.2. Thus, there is only 0.3 percent probability that the number of doublets should be less than 111 or greater than 163 if craters of doublets arise only from random single-body impact. The fact that 461 doublets are observed on the Martian surface suggests that most craters are not produced by random single-body impact.

The Monte Carlo result is further substantiated by a separate, analytic derivation showing the expected number of doublets produced by random single body impact as 141, this quantity is derived as follows: a pair of craters of radius $\underline{r}_1$, $\underline{r}_2$ whose centers are specified on some reference surface by the cartesian coordinates $(\underline{X}_1, \underline{Y}_1)$, $(\underline{X}_2, \underline{Y}_2)$ form a doublet if the relationship:

$$\underline{r}_1 + \underline{r}_2 - \Delta \leq \left[(X_1 - X_2)^2 + (Y_1 - Y_2)^2\right]^{1/2} \leq r_1 + r_2 + \Delta \qquad (2)$$

is satisfied where Δ denotes the allowable overlap or separation of crater rims. This relationship is schematically shown in Figure 6. The area denoted by $\underline{A}_0$ in the figure defines the region within which the center of crater 2 must lie in order to form a doublet with crater 1 and is given by: Fig. 6

$$\underline{A}_0 = \pi(\underline{r}_1 + \underline{r}_2 + \Delta)^2 - \pi(\underline{r}_1 + \underline{r}_2 - \Delta)^2 = 4\pi\Delta\,(\underline{r}_1 + \underline{r}_2) \qquad (3)$$

It is clear that for given values of $\underline{r}_1$, $\underline{r}_2$, and Δ, the probability of two randomly distributed craters forming a doublet is given by

$$\underline{P}\,(\underline{r}_1, \underline{r}_2, \Delta) = \frac{\underline{A}_0}{\underline{A}_{\underline{r}}} = \frac{4\pi\Delta\,(\underline{r}_1 + \underline{r}_2)}{\underline{A}_{\underline{r}}} \qquad (4)$$

where $\underline{A}_r$ is given as 3.397×10^6 km. From a probabilistic standpoint, each crater radius is between 2.0 km and 125.25 km characteristic of the 906 craters used in this study. On the average, however, two randomly chosen craters are expected to have radii equal to the mean radius, denoted here by $\underline{E}(\underline{R})$, of the 906 craters. Similarly, Δ may assume any value between 0 km and 12.5 km characteristic of the 461 crater pairs whose empiric separation or overlap is less than or equal to 12.5 km. Thus, again on the average, it is expected that a randomly chosen Δ is expected to have a value equal to the mean Δ, denoted by ΔM, of the 461 crater pairs. Substituting $\underline{E}(\underline{R})$ for $\underline{r}_1$ and $\underline{r}_2$ and ΔM for Δ in equation (4) then gives:

$$\underline{P}_0 = \frac{8\pi \ \Delta\underline{M} \ \underline{E}(\underline{R})}{\underline{A}_{\underline{r}}} \tag{5}$$

the probability that an arbitrarily chosen pair of randomly distributed craters form a doublet. Moreover, since there are $\binom{906}{2}$ possible crater pairs, the expected number of doublets among 906 randomly distributed craters is given by

$$\underline{E}(\underline{D}) = \binom{906}{2} \ \underline{P}_0 \tag{6}$$

or

$$\underline{E}(\underline{D}) = \binom{906}{2} \ \frac{8\pi(\Delta\underline{M})\underline{E}(\underline{R})}{\underline{A}_{\underline{r}}} \tag{7}$$

Estimates of $\underline{E}(\underline{R})$ and ΔM, respectively, may be obtained from values of the arithmetic mean radius of 10.25 km exhibited by the 906 craters used in this study and the mean Δ of 4.53 km exhibited by the 461 crater pairs. Substitution of these values for E(R) and ΔM into equations (6) and (7) yields E(D) = 140.8. This result agrees well with the mean number of doublets (137) produced by the 150 Monte Carlo simulations and is evidence that many of the observed 461 doublets have been produced by a nonrandom process.

Figure 5b shows the number of Mars doublets and the average and standard deviations of the numbers of Monte Carlo doublets as a function of ratio of largest doublet member radius to smallest doublet member radius. The distribution of Martian doublet ratios differs most from the Monte Carlo distributions for $\underline{R}_{max}/\underline{R}_{min}$ intervals nearest 1. Examination of doublets characterized by these values of $\underline{R}_{max}/\underline{R}_{min}$ should reveal the greatest number of doublets whose individual members were produced by the nonrandom cratering process. Study of all doublets with these ratios show that many of the craters of a given doublet are of the same freshness, a result that is unlikely if the individual craters were produced by separate impact. Another unique characteristic of these craters is that when overlap occurs one crater wall is seldom breached by the other. Instead, the craters seem to share a common wall, which appears many times to be straight as for crater doublets 1, 2, 4, and 5.

When $\underline{R}_{max}/\underline{R}_{min}$ values are large, the distribution of Martian doublets with a given value of $\underline{R}_{max}/\underline{R}_{min}$ may also differ from that observed with the Monte Carlo simulation. These Martian doublets are typically combined with other doublets such

that the large member is often common to many of the doublets. Because of the great difference in crater diameter for these doublets, and therefore a variation in weathering rates, it is impossible to judge the relative age of doublet members. The unique characteristic of this group of doublets is that they often have the same common larger central member; that is, satellite craters occur on the rim of a large central crater. An example is crater 13, which has many satellite craters (Figure 2).

ORIGIN OF NONRANDOM DOUBLET CRATERS AND CRATER CLUSTERS

Martian Calderas

The origin of large terrestrial and lunar craters has usually been attributed to volcanic or impact processes. Of the volcanic processes, often proposed as the cause of nonrandom crater distributions, the only mechanism that seems likely to produce craters even comparable in size to the Martian doublet craters is engulfment of roofs of large magma chambers. This can occur following eruption or withdrawal of large quantities of magma. Such eruption can be massive and rapid from a central conduit as it was for Krakatoa, or it can occur less rapidly from lateral fissures as in the Valles type caldera [Williams, 1968]. Collapse of large crustal blocks can even occur coincident with lateral intrusion as exemplified by the Glencoe type caldera [Williams, 1968]. However, craters resulting from such volcanic activity usually are not circular because they are products of collapse and thus reflect local rock inhomogeneities. One property of calderas is that the rims are often scalloped due to collapse of lateral pockets of magma. Other irregularities exist such as radial grabens. Neither of these

features has been observed for the Martian craters. Furthermore, and most important, small calderas are not usually circular, and terrestrial calderas equal to the median size of the Mars craters are usually volcano-tectonic depressions; many do not even resemble Mars craters, for their shapes are controlled by pre-existing basement structures and they are often irregular oblong or even rectangular depressions [Williams, 1968].

From various circularity indexes of terrestrial impact craters and calderas and lunar craters Murray [1969] concluded that many lunar craters are of impact origin. One circularity index used by Murray is the ratio of largest diameter to smallest diameter measured through the crater center of gravity. This index was obtained here for Mars craters; isolated craters were measured as well as separated members of doublets and clusters. Overlapping craters were not included because they would not be circular even if they were produced by the impact process. Results of these measurements are shown in Figure 7. Data Fig. 7 from terrestrial calderas (closed circles) were taken from Murray [1969]; data for Martian craters are shown as solid circles. Even with distortion present on Martian photographs, which results in overestimates of the circularity index, the mean values for Martian craters are considerably less than those for terrestrial calderas. The difference is greatest for large craters because for terrestrial calderas departure from circularity increases with crater size. These results suggest that the Martian doublets and crater clusters are not calderas—unless rock properties are much different on Mars than on Earth, which seems unlikely.

Crater Doublets Produced by Tidal Splitting of Meteoroids

The plausibility of tidal splitting and separation as a means of Mars doublet formation was examined in terms of the meteoroid mass, tensile strength, entry velocity, and entry angle required to produce a crater doublet with crater diameters $\underline{D}_1$ and $\underline{D}_2$.

Sekiguchi [1970] shows that tidal forces may split a large meteoroid into two fragments of approximately equal size. The fragmentation altitude $\underline{h}$ in terms of the meteoroid radius $\underline{a}$ and tensile strength $\underline{T}$ is shown for impact on Mars in Figure 8 and is given by: Fig. 8

$$\underline{h} = \underline{R}_0 \left\{ \left[\frac{57}{64} \left(\frac{2}{3} + \frac{T}{f \pi \rho^2 a^2} \right) \right]^{-1/3} - 1 \right\} \qquad (8)$$

where $\rho = 3.95$ gm/cc is the mean density of Mars and $R_0 = 3393.4$ km is the planet radius; $\underline{a}$ is the meteoroid radius and $\underline{f}$ is the gravitational constant. Inspection of Figure 8 shows that if meteoroids have tensile strength characteristic of hand samples of silicate rocks ($\cong 10^8$ dynes/cm^2) then most of the bodies of the size required for forming the Martian doublets (< 20 km diameter) will not be split by tidal forces. However, it is probable that large meteoroids are characterized by tensile strength much less than 10^8 dynes/cm^2. Even hand samples of some meteoroids such as carbonaceous chondrites are very friable and would possess tensile strength of less than about 10^7 dynes/cm^2. However, the strength of large meteoroids should be significantly reduced from this value due to the presence of large defects or cracks. These would certainly be present if

meteoroids have resulted from breakup of a parent body caused by collision [Mason, 1970]. Even if the large meteoroids formed as separate bodies, large cracks should be present. Differential thermal contraction of different rock forming minerals produces stresses which commonly fractures new rock formation on earth.

According to Griffith [1921], there is a basic relationship between compressive or tensile strength and the length of cracks in any brittle material. The crack length can be of atomic dimensions or longer. The theory has been used to explain the observed reduction of material strength with increasing size for samples small enough to be measured in the laboratory [Brace, 1961]; it appears to be valid for large-scale applications as well. Brace has shown that a modification of the Griffith theory is equivalent to the Coulomb law of failure, which is the basis of the Anderson theory of geologic faulting. According to Brace [1961], the applied tensile stress at fracture can be calculated from:

$$\underline{T} = \left(\frac{2\underline{E}\underline{S}}{\pi \underline{a}}\right)^{1/2} \tag{9}$$

where $\underline{E}$ is Young's modulus (dynes/cm^2), $\underline{S}$ is specific surface energy of the material in ergs/cm^2 and $\underline{a}$ is the half crack length of the Griffith crack in cm.

For simplicity, we compute the dependence of tensile strength of rocks as a function of the hypothetical crack length from equation (9). Following Brace [1961], we assume a value of 10^3 ergs/cm^2 for $\underline{S}$ of most rocks and a value of 10^{12} dynes/cm^2 for Young's modulus. Figure 9 shows the calculated relationships that result. Note that the calculated tensile strength for crack length equal to the

Fig. 9

grain size of most rocks (without large-scale cracks) is in basic agreement with typical observed values of $\underline{T} \cong 10^8$ dynes/cm^2 for hand samples. Meteoroids with this tensile strength of the size required to form doublets ($\leq$ 20 km) would never be split by the gravitational field of Mars. However, any cracks present of the order of 10 meters in length (1/100 or less the size of the body) can reduce the tensile strength of the meteoroid to 10^5 to 10^6 dynes/cm^2. A meteoroid $\leq$ 20-km-diameter with this tensile strength will fail at high altitudes above Mars (Figure 8). Thus, Sekiguchi's model for meteoroid breakup [eq. (8)] predicts reasonable values of breakup altitude as a function of meteoroid radius and tensile strength for meteoroids impacting Mars—providing large cracks are present in meteoroids. It may be that if cracks are large enough, $\underline{T}$ approaches 0 and the altitude of breakup would be more accurately approximated by the Roche limit. It is noted that if equation (8) is solved for $\underline{T} = 0$, we do not obtain the Roche limit. Consideration of the relationship between the Roche limit and Sekiguchi's breakup altitude for nearly collisionless bodies is beyond the scope of this paper. However, Sekiguchi's result is based on Kelvin's study of tidal forces on the earth in an earth, moon, sun system in equilibrium. Strictly speaking a two body system should have been developed for the fission model. This model would yield higher breakup altitudes and greater numbers of doublets than that reported here.

Certain conditions of impact velocity and impact angle are required for separation of the fission products and formation of craters of the correct diameters for production of nearly tangential craters. From the equations of motion of the fission products, Sekiguchi shows that the distance of separation of the impact points, $\Delta\underline{x}$, on the planetary surface is given by:

$$\Delta \underline{x} = \Delta \underline{z} \cosh (\gamma \underline{t}) \tan \Theta \qquad (10)$$

where:

$$\gamma = \left(\frac{2 \underline{f} \underline{M}}{\underline{R}^3} \right)^{1/2}$$

Θ = impact angle from Mars surface normal

$\underline{M} = 6.455 \times 10^{26}$ gm = mass of Mars

$\underline{R}$ = 3,393.4 km = radius of Mars

$\underline{F} = 6.664 \times 10^{-8}$ dyne cm^2 gm^{-2} = gravitational constant

$\Delta \underline{z}$ = parent impacting body radius

$\underline{t}$ = time of flight (sec) from breakup to impact

This equation is not the same as that given by Sekiguchi but it is correct. Sekiguchi's eq. 5.3 results from a typographical error in the solution for the differential equation of motion of the fission products. Equation (10) can be modified to yield $\Delta \underline{x}$ in terms of crater diameters $\underline{D}_1$ and $\underline{D}_2$ produced by the fission products of masses $\underline{M}_1$ and $\underline{M}_2$. For impact on this scale, we may assume that craters produced by shallow depth of burst explosions simulate impact crater formation [Baldwin, 1963; Oberbeck, 1971]. One of Baldwin's [1963] equations for shallow depth of burst explosion craters can be modified to express crater formation energy in ergs and crater diameter in cm:

$$\log \underline{E} = \frac{\log \underline{D}_E + 2.924}{0.3284} \qquad (11)$$

where $\underline{E}$ is crater formation energy in ergs and $\underline{D}_E$ is terrestrial crater diameter in cm. Expressing $\underline{D}_E$ in terms of equivalent diameter on Mars ($\underline{D}_M$) for the same impact energy, we obtain from Johnson's [1970] experimental results:

$\underline{D}_{\underline{E}} = \underline{D}_{\underline{M}}\left(\frac{\underline{g}_{\underline{M}}}{\underline{g}_{\underline{E}}}\right)^{.12}$ where $\underline{g}_{\underline{M}}$ and $\underline{g}_{\underline{E}}$ are the acceleration of gravity on Mars and Earth, respectively. Substituting this value into equation (11) and taking antilogs yields in cgs units:

$$E = 5.59 \times 10^8 \, D_M^{3.045} \tag{12}$$

The relationship is valid only for vertical impact where all available energy is used for cratering. There is evidence that the energy of formation of cratering is given by the product of the cosine of the impact angle measured from the surface normal and the projectile kinetic energy [Moore, 1971]; we modify equation (12) to take account of impact angle and equate energy of formation to the product of cosine of impact angle and projectile kinetic energy to yield meteoroid mass $\underline{M}$:

$$\underline{M} = 11.18 \times 10^8 \, \underline{D}^{3.045}/(\underline{V}^2 \cos \theta) \tag{13}$$

where $\underline{V}$ is impact velocity and θ is impact angle from the Mars surface normal. This expression and the assumption of spheroidal shape and ρ of meteoroid = 3.4 gm/cc for the parent body can be used to yield a relationship between parent body radius $\Delta\underline{z}$ and doublet crater diameters $\underline{D}_1$ and $\underline{D}_2$ that would be produced from the fission products of breakup of a parent body of radius $\Delta\underline{z}$:

$$\Delta\underline{z} = \frac{4.32 \times 10^2 \, (\underline{D}_1^{3.045} + \underline{D}_2^{3.045})^{1/3}}{\underline{V}^{2/3} \cos^{1/3} \theta} \tag{14}$$

Substitution for $\Delta\underline{z}$ in equation (10) yields $\Delta\underline{x}$, the separation distance of centers of the craters in terms of $\underline{D}_1$, $\underline{D}_2$, $\underline{V}$, θ, $\underline{M}$, $\underline{R}$ and flight time $\underline{t}$:

$$\Delta x = \frac{4.32 \times 10^2 \left(\underline{D}_2^{3.045} + \underline{D}_2^{3.045}\right)^{1/3} \cosh(\gamma \underline{t})}{\underline{V}^{2/3} \cos^{1/3}\theta \cot\theta} \tag{15}$$

Finally, division of both sides of this equation by $(\underline{D}_1 + \underline{D}_2)/2$, the average crater diameter, yields a separation ratio $\underline{y}$, the ratio of distance between crater centers to average crater diameter:

$$y = \frac{\Delta x}{(\underline{D}_1 + \underline{D}_2)/2} = \frac{8.64 \times 10^2 \left(\underline{D}_1^{3.045} + \underline{D}_2^{3.045}\right)^{1/3} \cosh(\gamma \underline{t})}{\underline{V}^{2/3} \cos^{1/3}\theta \cot\theta \, (\underline{D}_1 + \underline{D}_2)} \tag{16}$$

Equation (16) can be used to determine the relationship between impact angle of the parent body and ratio of separation between crater centers to average crater diameter for craters produced at the same impact velocity from the fission products of breakup at a given altitude. This is accomplished by first measuring $\underline{D}_1$ and $\underline{D}_2$ of craters forming a given doublet. These values are substituted into equation (16), and θ is varied for constant values of $\underline{V}$ to compute the separation ratio as a function of impact angle θ. Flight time $\underline{t}$, required in equation (16) for each solution for $\underline{y}$, is computed from each value of $\underline{V}$, θ, and altitude of meteoroid breakup. Altitude of breakup is computed from equation (8), which requires knowledge of tensile strength $\underline{T}$ and meteoroid radius $\underline{a}$. Meteoroid radius $\underline{a}$ is equal to $\Delta \underline{z}$ where $\Delta \underline{z}$ is given by equation (14) and the values assumed for $\underline{V}$ and θ; $\underline{T}$ is calculated from equation (9) by assuming that the largest crack length is always .02 $\underline{a}$. Figure 10$\underline{a}$ shows these solutions for the largest isolated observed crater doublet where $\underline{D}_1$ = 68.5 km and $\underline{D}_2$ = 86.2 km. Examination of this figure shows that doublet formation ($\underline{y} \cong 1$)

Fig. 10

occurs primarily for high entry angles, θ. Similar solutions have also been obtained for doublets with smaller average diameters and for different assumed ratios of defect length to meteoroid diameter. The fact that doublet formation is restricted to bodies impacting at high angles to the surface normal seems at first consideration incompatible with the observation that of the total of 906 craters there are 461 doublets. However, many doublets occur in the same crater cluster and could have resulted from breakup of a single body. To more accurately approximate the number of impacting bodies that could have been broken up, doublets and clusters have been counted as single breakup events. If isolated craters are also counted as single impact events, we find that as small a fraction as 3/10 of the impacting bodies could have broken before impact. This result is in better agreement with the theoretical results of Figure 10, but it is still higher than expected. Some of the doublets or clusters counted as single events could have been produced by a number of separate impacts. Also, the theoretical model does not consider the effect of stress energy stored in the meteoroid or meteoroid rotation. Both effects would yield greater separation between fission products and more doublets. Thus, the observed number of doublets and clusters seems to be in fair agreement with the theoretical predictions of the fission model.

Estimates of the possible aerodynamic lifting forces were made and included in the calculation of tidal separation. In obtaining an estimate of the maximum separation due to aerodynamic lift, we ignore drag forces and make the simplifying assumptions that the velocity $\underline{v}$ and trajectory angle θ as measured to the normal are constant. According to Berman [1961], the lifting force normal to the trajectory is:

$$\underline{F}_2 = 1/2\ \underline{C}_\ell\ \underline{S}\rho\ \underline{V}^2 \tag{17}$$

where ρ is the atmospheric density, $\underline{C}_\ell$ is the lift coefficient, and $\underline{S}$ is the frontal cross section of the body. Then, we make the approximation $\underline{h} = \underline{h}_0 - \underline{v} \cos\theta\ \underline{t}$ or $\underline{dt} = -\underline{dh}/\underline{v} \cos\theta$, where $\underline{h}$ denotes the altitude, $\underline{t}$ is the flight time, and $\underline{h}_0$ denotes the altitude at $\underline{t} = 0$. Moreover, approximating the relationship between ρ and $\underline{h}$ [Berman, 1961] by

$$\rho = \rho_0\ \underline{e}^{-\beta \underline{h}} \tag{18}$$

where $\beta = 9.86 \times 10^{-7}$ and $\rho_0 = 1.33 \times 10^{-5}$ gm/cc [Levin et al., 1968], and performing a double integration, we obtain the displacement on the surface for a body as

$$\underline{X}_0 = \underline{e}^{-\beta \underline{h}_0} \left(\frac{1/2 \underline{C}_\ell \underline{S} \rho_0}{M \cos^3\theta \beta^2} \right) \left[e^{\beta(\underline{h}_0 - \underline{h}_b)} - \left(\left[\underline{h}_0 - \underline{h}_b \right] \beta - 1 \right) \right] \tag{19}$$

where $\underline{M}$ = meteoroid mass, $\underline{S}$ = meteoroid cross section, and $\underline{h}_b$ = altitude of breakup. We then estimate the maximum separation between two meteoroids as $2\underline{X}_0$. Separation due to tidal splitting and aerodynamic lift is shown as a solid line for each velocity in Figure 10. Aerodynamic lift has little effect on separation due to the tenuous Martian atmosphere.

DISCUSSION

It is highly probable that a nonrandom cratering effect has contributed to the production of the cratered terrain on the planet Mars. It is conceivable that some

of the isolated nonrandomly produced doublets could have been produced by simultaneous impact of gravitationally coupled asteroids. Tanner [1963] has shown that such coupled bodies could remain stable as they impact the Earth. Since it has been shown in this study that meteoroids approaching Mars could produce the observed doublets, if meteoroids are large enough, meteoroid fission due to stresses induced by the gravitational field of Mars is favored at this time for the nonrandom production of doublets or crater clusters.

If the Mars doublets have been produced by simultaneous impact of meteoroids, it is reasonable to expect the development of unusual features due to close proximity of formation of one crater relative to the other. Doublet craters have been produced in sand targets in the laboratory both by separate and simultaneous impact of two halves of a cylinder that has been partially severed before launch. Complete severing and separation of the cylinder halves occurs as a result of spinning induced by rifling in the gun barrel. For doublets produced by simultaneous impact, both pieces of the cylinder are allowed to impact. For doublets, produced by separate impact, one-half of the cylinder is captured and one crater is produced. Then, on the next firing the other half is caught and the other doublet member is produced. Degree of overlap is specified by the ratio of the separation between crater centers to diameter of either member crater ($\underline{S}/\underline{D}$). Figure 11 shows six doublets produced experimentally; three were formed at the specified values of S/D by simultaneous impact of half cylinders and three were formed by separate impact. All doublets were produced at about the same impact velocity of 2.3 km/sec. One interesting result is that the crater wall of one member of a doublet is breached by the other member only for those doublets whose members have been formed

Fig. 11

separately. This is illustrated by the doublets formed simultaneously and separately at nearly equal values of $\underline{S}/\underline{D}$ = 0.81 and 0.72, respectively. The last crater to form the doublet produced by separate impact partially destroyed and distorted the rim of the first crater. However, the crater rims of members of the doublet produced by simultaneous impact are equally developed. Another interesting feature of doublets produced by simultaneous impact ($\underline{S}/\underline{D}$ = 0.81) is that the common crater wall is straight and very high. A continuation of this wall projects onto the target surface so that there is a ridge perpendicular to the bilateral axis of symmetry of the doublet. Observations of growing craters shows that this is the product of focusing of the ejecta and extreme target deformation. For the doublet where the members are widely separated ($\underline{S}/\underline{D}$ = 1.3), the ridge occurs as a delicate subdued structure exactly midway between the separated members. Although exact modeling of the very large Mars doublets is not assumed or expected, the observations of resulting structures applied to Mars craters may support the theory of impact origin. Most isolated Mars doublets are characterized by craters that are equally developed, and the common walls of many doublets are straight and raised, as in doublets 4 and 5 in Figure 2. This may be of special significance because rims of isolated craters usually are not well developed on Mars, suggesting strong erosive processes. Focused secondary crater fields and ridges are present perpendicular to the bilateral axis of symmetry of the doublets produced in the laboratory, but these have not been observed for Mars doublets. However, focused secondary crater fields and ridges may have been subdued by erosion. It may be possible to observe remnants of such ridges and focused ejecta fields on higher resolution photographs that will soon be available.

The results of this study are of considerable importance to current and recent interpretations of the geologic history of Mars and the Moon based on observation of Mars cratering density compared to that of the Moon. It has been assumed [Murray, 1971] that Mars craters are the results of random single-body impact, contrary to the results presented here. On the basis of this assumption and the observed smaller ratio of large Martian craters to small craters on Mars as compared to the Moon, Murray concludes that the smaller bodies impacting the Moon could be from a different population than those impacting Mars and that the paucity of large fresh craters could be the result of an unusually efficient erosive process. Both hypotheses may not be true. The observations might be explained by the fact that fission of meteoroids appears to be common for impact on Mars, and this effect would certainly be less pronounced for impact on the Moon because of its smaller gravitational field. Thus, the observed deficiency of large fresh Mars craters compared to the Moon could be easily explained by the fact that more large bodies may be broken up to produce small craters on Mars than are broken up for impact on the Moon. Interpretations based on crater frequency alone are only valid when the crater distributions are random and when impact mechanisms are the same.

If the occurrence of nonrandom crater doublets on the surfce of Mars is explainable by the fission model, a new and unexpected aspect of the mechanics of planetary impact cratering has been revealed by the Mariner photographs. Meteoroids larger than some limiting diameter, dependent on the amplitude of the gravitational field of the planet and meteoroid tensile strength, might be broken up before impact. Thus, conditions on one planet may be more favorable to doublet and crater cluster development than on other planets. Other factors such

as the role of aerodynamic effects may also influence the number of doublets produced.

There are at least three possible terrestrial doublets that may have been produced by splitting due to stresses induced in impacting meteoroids by the gravitational field of the Earth. The Clearwater Lakes craters have already been described. The Rieskessel and the Steinheim Basin may be members of another doublet that are more widely separated than the members of the Clearwater Lakes craters. The Odessa and Meteor craters may constitute another widely separated pair.

Finally, we can tentatively suggest that the puzzling concentration of large mare impact basins on the Earth-facing side of the Moon, a pronounced large-scale example of a nonrandom effect, might in fact be the product of breakup of a large impacting body. Such a large body would certainly contain defects large enough to reduce the tensile strength to a point where the body is essentially cohesionless. In that case, breakup would occur near the Roche limit (2.44 times the Moon's radius). Alternatively, the body may have passed close enough to the Earth to have been ruptured by the earth's gravitational field. The products of breakup might well be a cluster of large impact basins with slight age differences that appear greater due to the domination in growth of one basin over others.

REFERENCES

1. Baldwin, R. G., The Measure of the Moon, 488 pp., University of Chicago Press, Chicago, 1963.
2. Berman, A. I., The Physical Principles of Astronautics, 350 pp., John Wiley and Sons, Inc., N. Y. - London, 1961.
3. Brace, W. F., Dependence of Fracture Strength of Rocks on Grain Size, Penn. State Univ. Mineral Industries Expt. Sta. Bull. No. 76, pp. 99-103, 1961.
4. Dence, M. R.; M. J. S. Innes; and C. S. Beals, On the Probable Meteoritic Origin of the Clearwater Lakes, Quebec, The Journal of the Royal Astronomical Society of Canada, 59, No. 1, 13, 1965.
5. Fassone, C., and S. Orthman, A Test Program for Pseudo-random Numbers with Uniform Distributions, European Atomic Energy Community, Joint Nuclear Research Center - Ispra Establishment (Italy) Scientific Information Processing Center, Brussels, May 1967, 80 pp.
6. Griffith, A. A., The Phenomena of Rupture and Flow in Solids, Phil. Trans. Roy. Soc. London, A, 221, 163, 1921.
7. Johnson, S. W.; J. A. Smith; E. G. Franklin; L. K. Moraski; and D. J. Teal; Gravity and Atmospheric Pressure Effects on Crater Formation in Sand, J. Geophys. Res., 74, 4838, 1969.
8. Levin, G. M.; P. E. Pitts; D. K. Weidner; V. I. Stevens; G. P. Wood; R. M. Henry; G. F. Campen; R. A. Schiffer; and H. B. Talifson, Models of Mars Atmospheres (1967), NASA SP-8010, 1968.
9. Marsaglia, G., and T. A. Bray, One-line Random Generations and Their Use in Combinations, Boeing Scientific Research Laboratory Mathematical Note 551, 1968.

10. Mason, B., The Origin of Meteorites, J. Geophys. Res., 65, 2965, 1960.

11. Moore, H. J., Missile Impact Craters, J. Geophys. Res. (In Press).

12. Murray, B. C.; L. A. Soderblom; R. P. Sharp; and J. A. Cutts, The Surface of Mars, Part 1, Cratered Terrain, J. Geophys. Res., 76, 313, 1971.

13. Murray, J. B., and J. E. Guest, Circularities of Craters and Related Structures on Earth and Moon, Modern Geology, 1, 149, 1970.

14. Oberbeck, V. R., Laboratory Simulation of Impact Craters with High Explosives, J. Geophys. Res., (In press).

15. Sekiguchi, N., On the Fissions of a Solid Body under Influence of Tidal Force, with Application to the Problem of Twin Craters on the Moon, The Moon, 1, 429, 1970.

16. Tanner, R. W., The Orbital Perturbations of a Very Large Twin Meteorite, The Journal of the Royal Astronomical Society of Canada, 57, 109, 1963.

17. Williams, H., An investigation of Volcanic Depressions. Part 1: Geologic and Geophysical Features of Calderas, Oregon Univ. Progress Report, pp. 90, Jan. 22, 1968.

FIGURE CAPTIONS

Fig. 1. Photograph Clearwater Lakes Craters. Photograph courtesy of M. Dence.

Fig. 2. Mars chart showing location of photographs.

Fig. 3. Mars photographs with doublets outlined and labeled.

Fig. 4a. Cumulative size frequency distribution of craters on photographs 6N17, -19, -21, -23, and 7N25.

Fig. 4b. Cumulative number of doublets with overlap or separation distance greater than Δ, km.

Fig. 4c. Histogram of the number of observed doublets as a function of ratio of largest member diameter to smallest member diameter.

Fig. 5a. Distribution of number of doublets that form for 150 Monte Carlo simulations of Martian cratering.

Fig. 5b. Average and standard deviation of number of doublets formed in Monte Carlo simulation with indicated ratio of $\underline{R}_{max}/\underline{R}_{min}$ (solid lines). Same distribution for observed doublets, dashed line (from Figure 3c).

Fig. 6. Region within which the center of the second crater must be in order to form a doublet in the Monte Carlo simulation.

Fig. 7. Circularly indices of terrestrial calderas (closed circles) from Murray [1969], and circularity indices of Martian craters.

Fig. 8. Relationship between breakup altitude above the planet Mars and meteoroid radius for different assumed values of meteoroid tensile strength.

Fig. 9. Calculated relationship between tensile strength and "half crack length," for average silicate rock.

Fig. 10. Relationship between separation ratio and impact angle for values of impact velocity V = 5.15, 10, 20, and 25 km/sec; (a) tidal effects only and (b) tidal and aerodynamic effects.

Fig. 11. Crater doublets produced by separate and simultaneous production of doublet members.

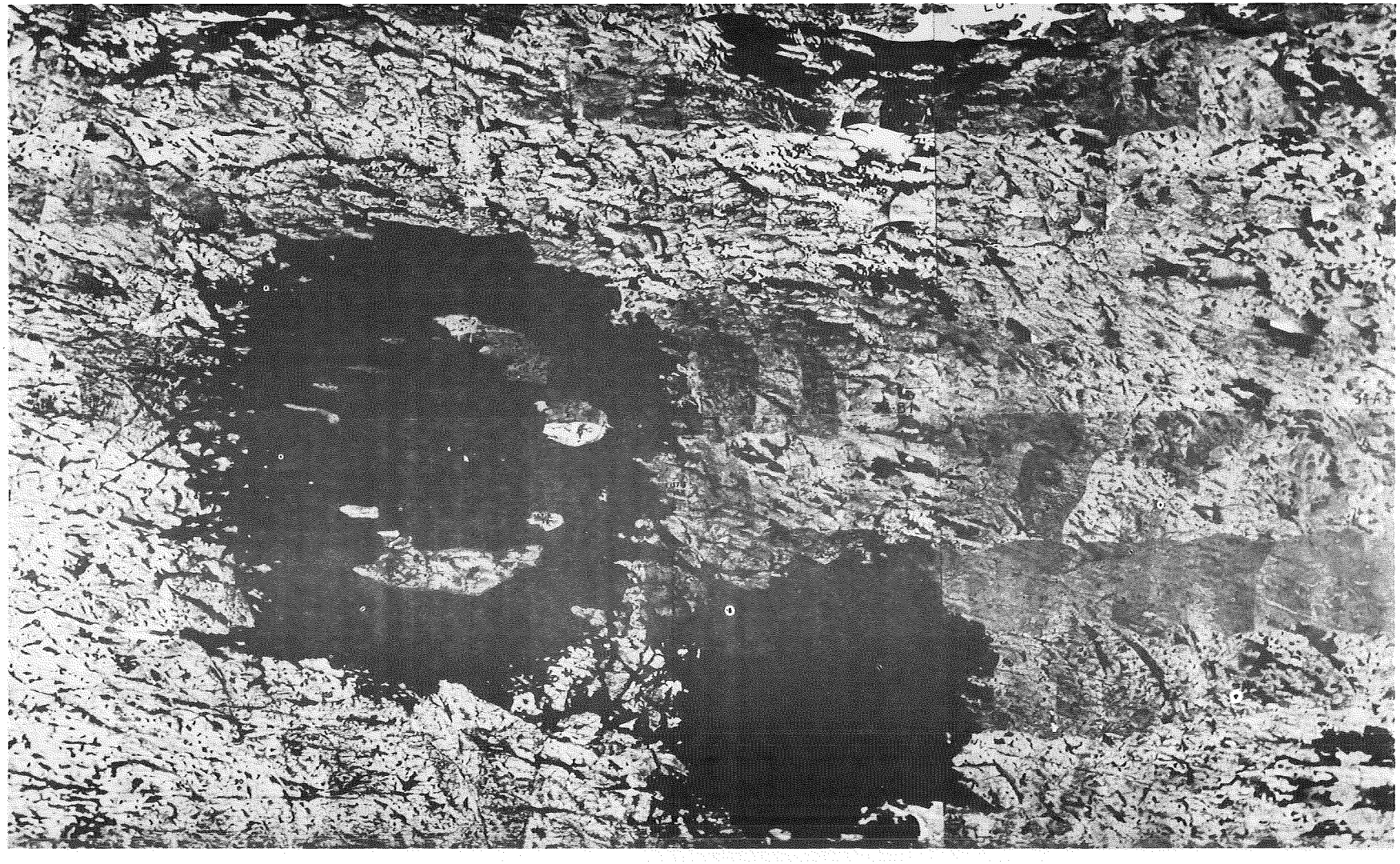

Figure 1.

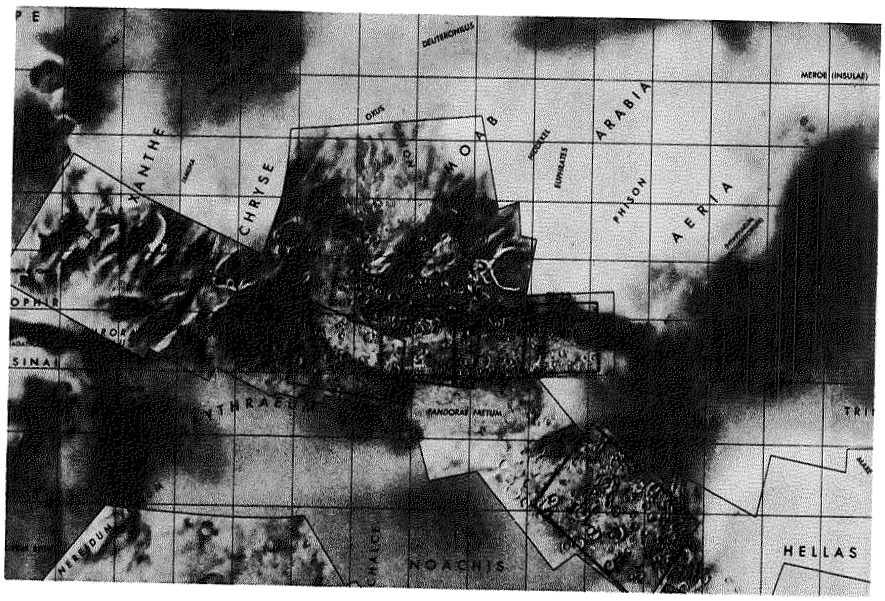
DELTA HORUS
MEROE (INSULAE)
ARABIA
AERIA
PHISON
CHRYSE
HELLAS
NOACHIS

Figure 2.

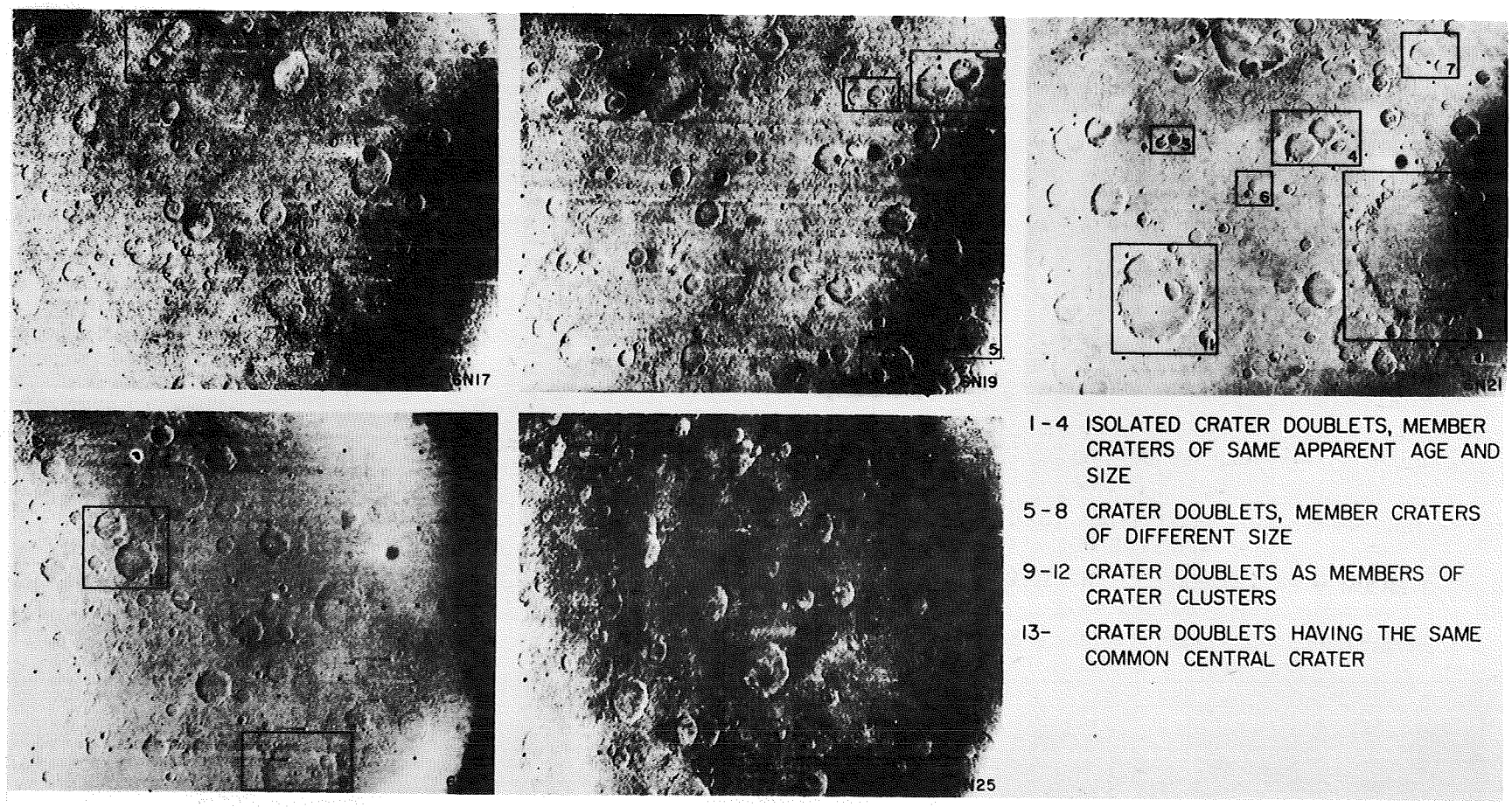
6N17
5
6N19
7
6
5
4
6
1
6N21
N25
1 - 4 ISOLATED CRATER DOUBLETS, MEMBER CRATERS OF SAME APPARENT AGE AND SIZE
5 - 8 CRATER DOUBLETS, MEMBER CRATERS OF DIFFERENT SIZE
9 - 12 CRATER DOUBLETS AS MEMBERS OF CRATER CLUSTERS
13- CRATER DOUBLETS HAVING THE SAME COMMON CENTRAL CRATER

Figure 3.

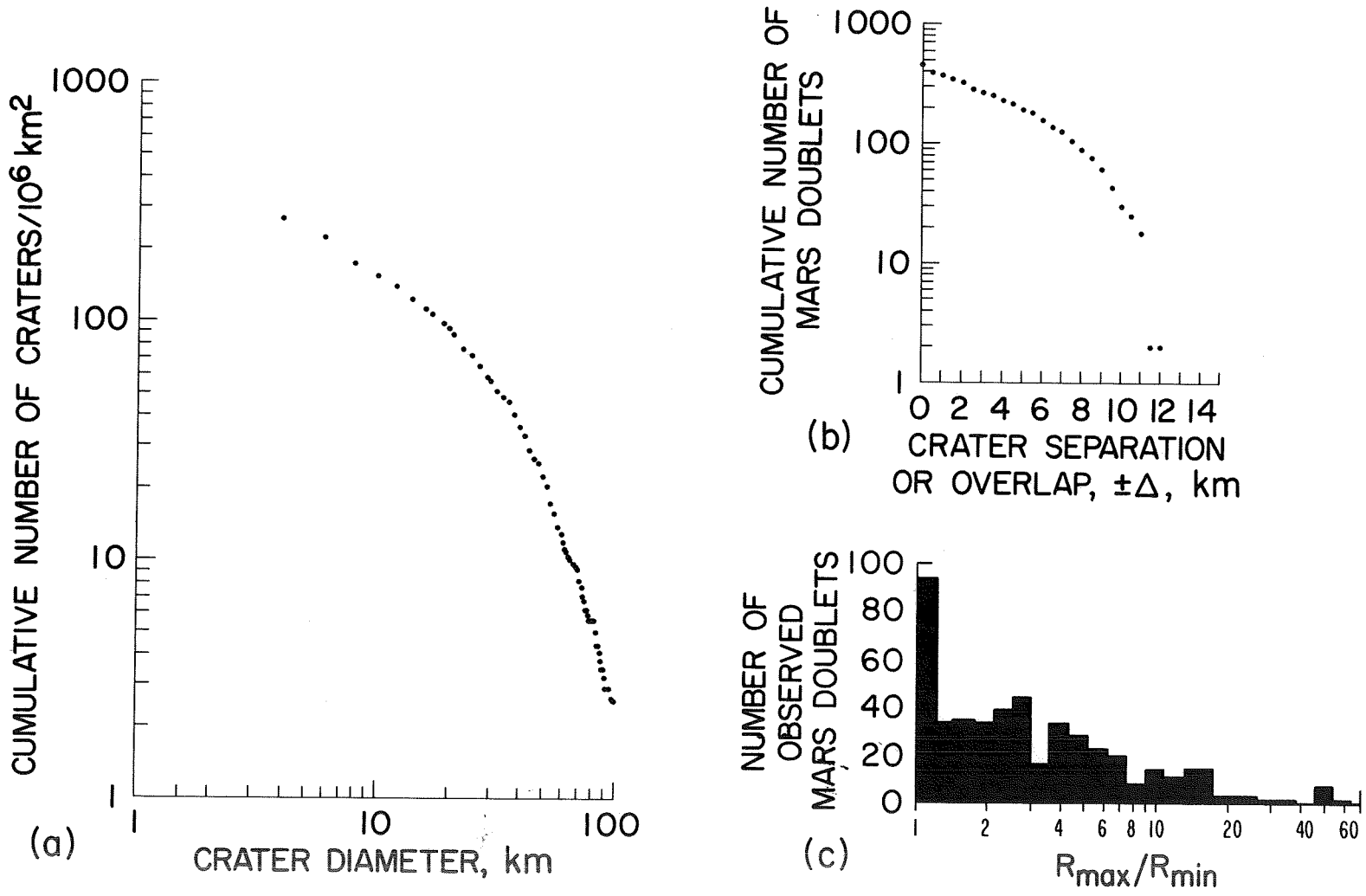
CUMULATIVE NUMBER OF CRATERS/10⁶ km²
1000
100
10
1
1
10
100
(a)
CRATER DIAMETER, km
CUMULATIVE NUMBER OF MARS DOUBLETS
1000
100
10
1
0 2 4 6 8 10 12 14
(b)
CRATER SEPARATION OR OVERLAP, ±Δ, km
NUMBER OF OBSERVED MARS DOUBLETS
100
80
60
40
20
0
1 2 4 6 8 10 20 40 60
(c)
Rmax/Rmin

Figure 4.

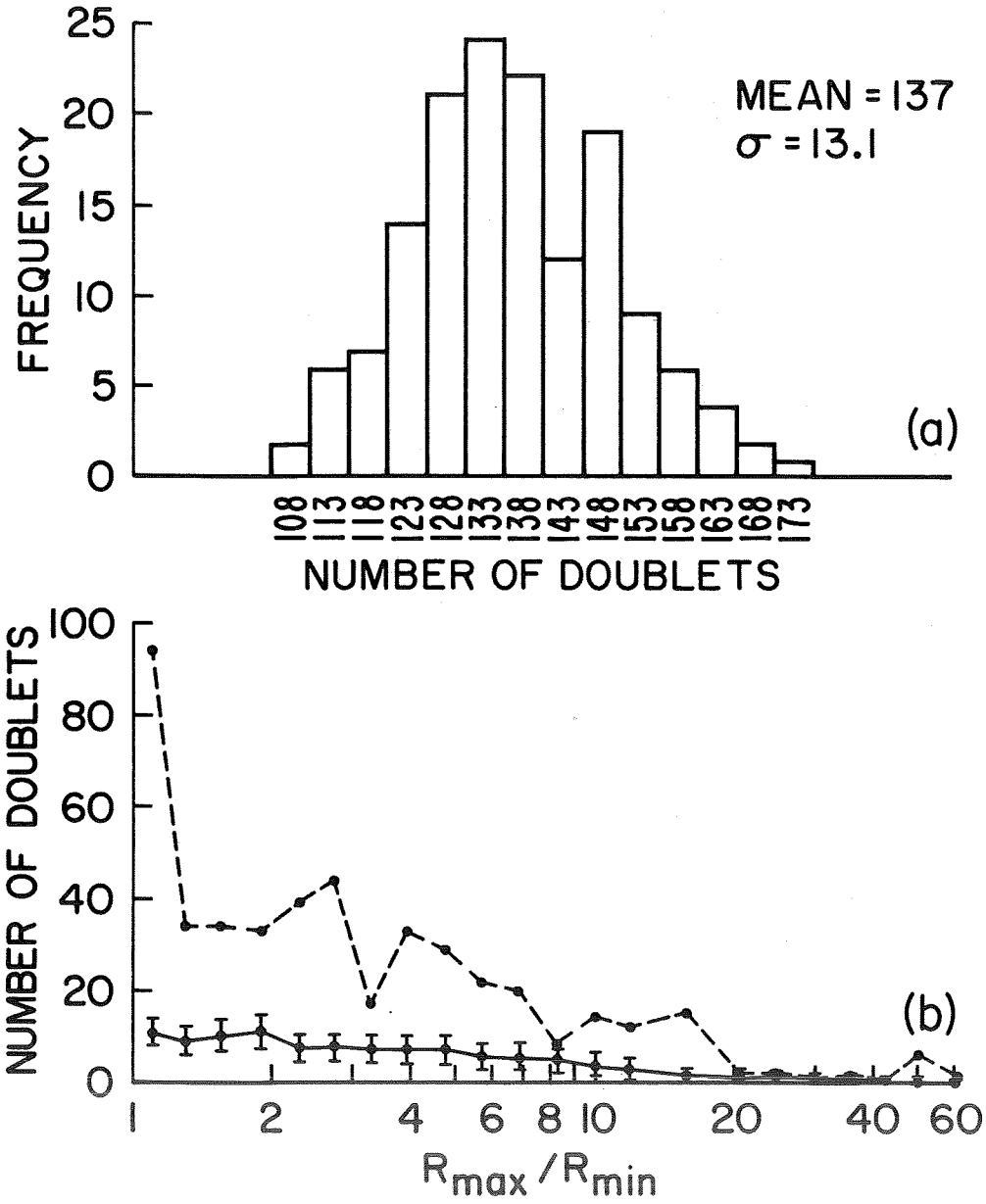
25
20
15
10
5
0
FREQUENCY
MEAN = 137
σ = 13.1
(a)
108
113
118
123
128
133
138
143
148
153
158
163
168
173
NUMBER OF DOUBLETS
100
80
60
40
20
0
NUMBER OF DOUBLETS
(b)
1
2
4
6
8
10
20
40
60
Rmax / Rmin

Figure 5.

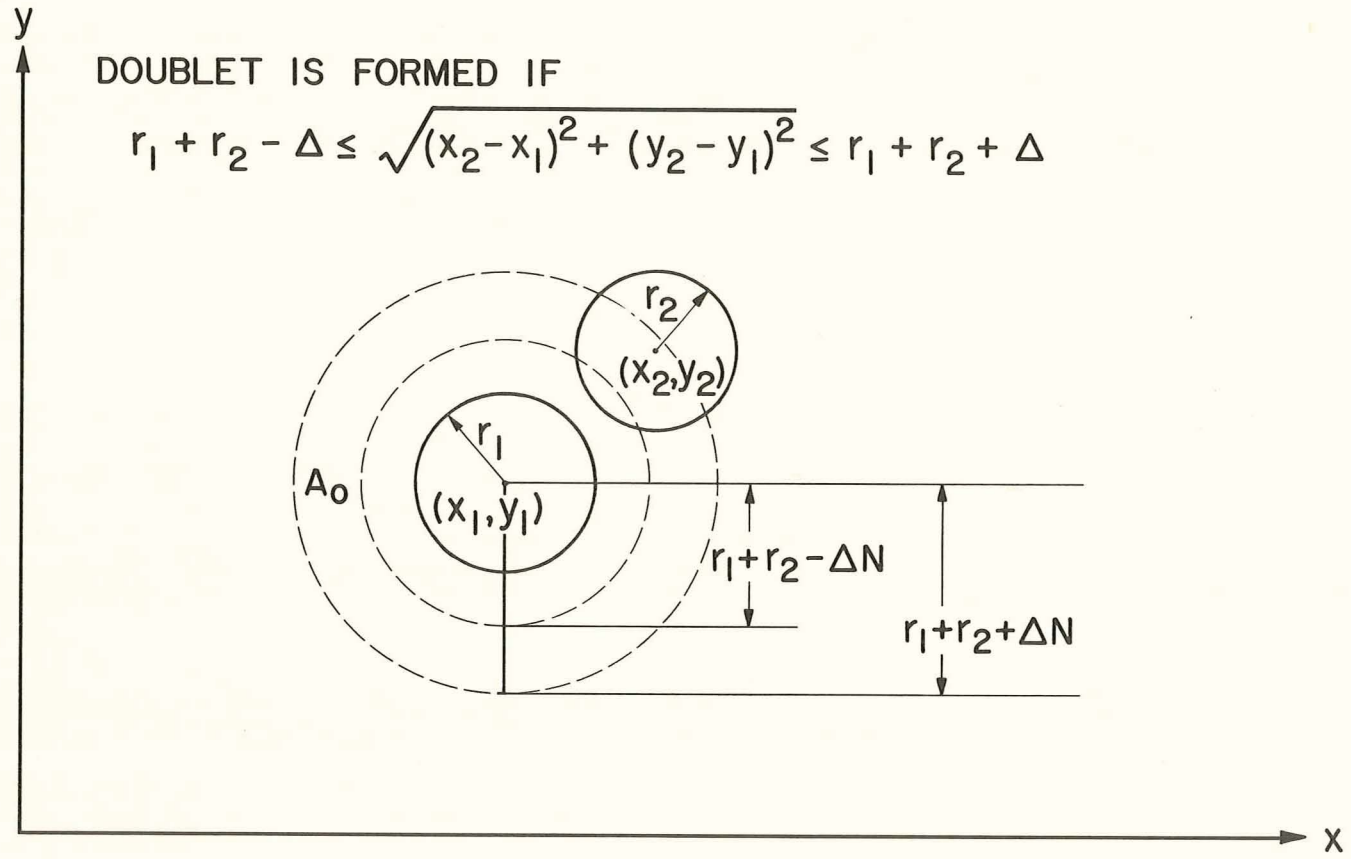
y
DOUBLET IS FORMED IF
$r_1 + r_2 - \Delta \leq \sqrt{(x_2-x_1)^2 + (y_2-y_1)^2} \leq r_1 + r_2 + \Delta$
r_2
(x_2,y_2)
r_1
A_o
(x_1,y_1)
$r_1+r_2-\Delta N$
$r_1+r_2+\Delta N$
x

Figure 6.

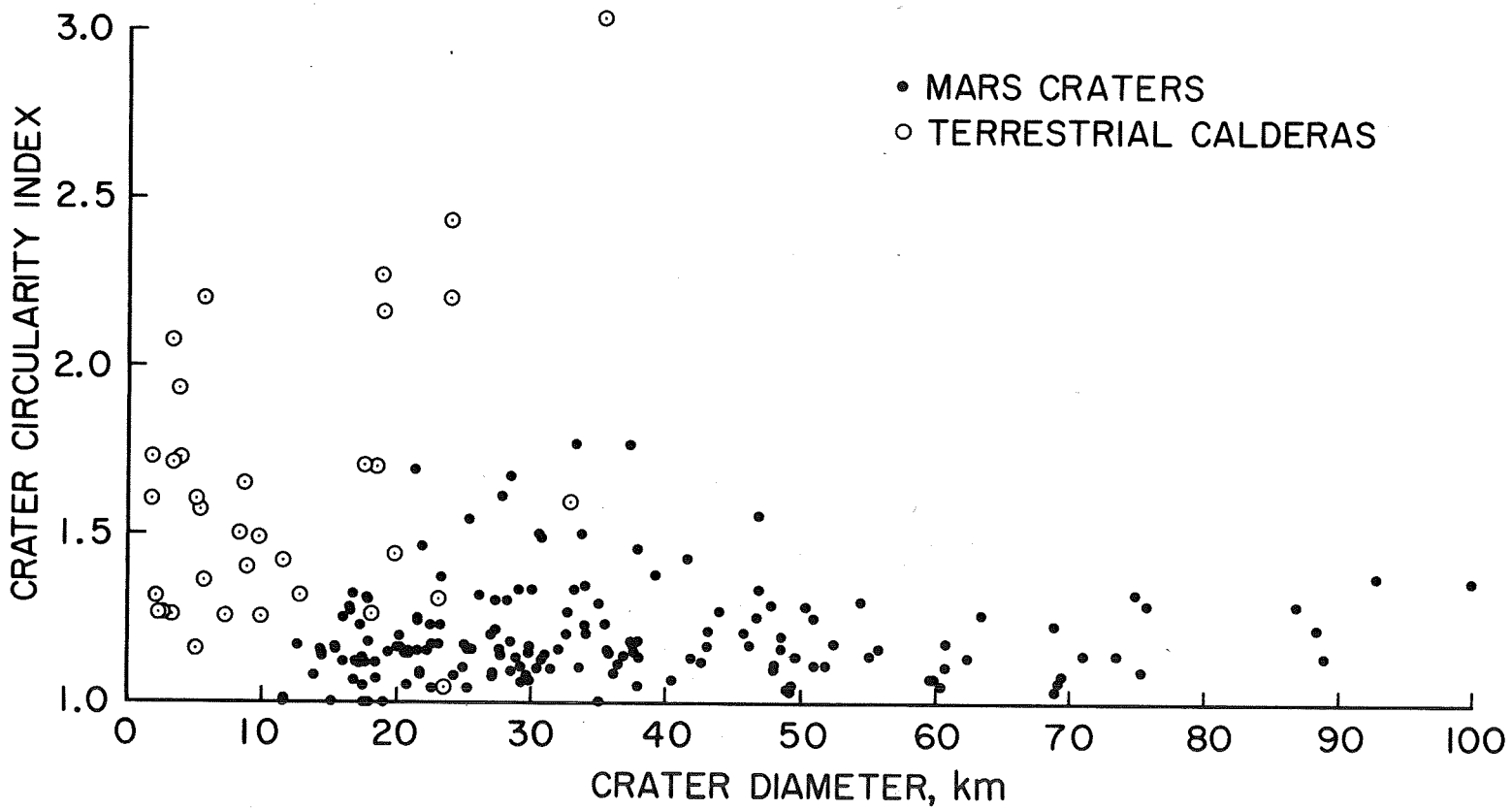
3.0
2.5
2.0
1.5
1.0
CRATER CIRCULARITY INDEX
• MARS CRATERS
○ TERRESTRIAL CALDERAS
0
10
20
30
40
50
60
70
80
90
100
CRATER DIAMETER, km

Figure 7.

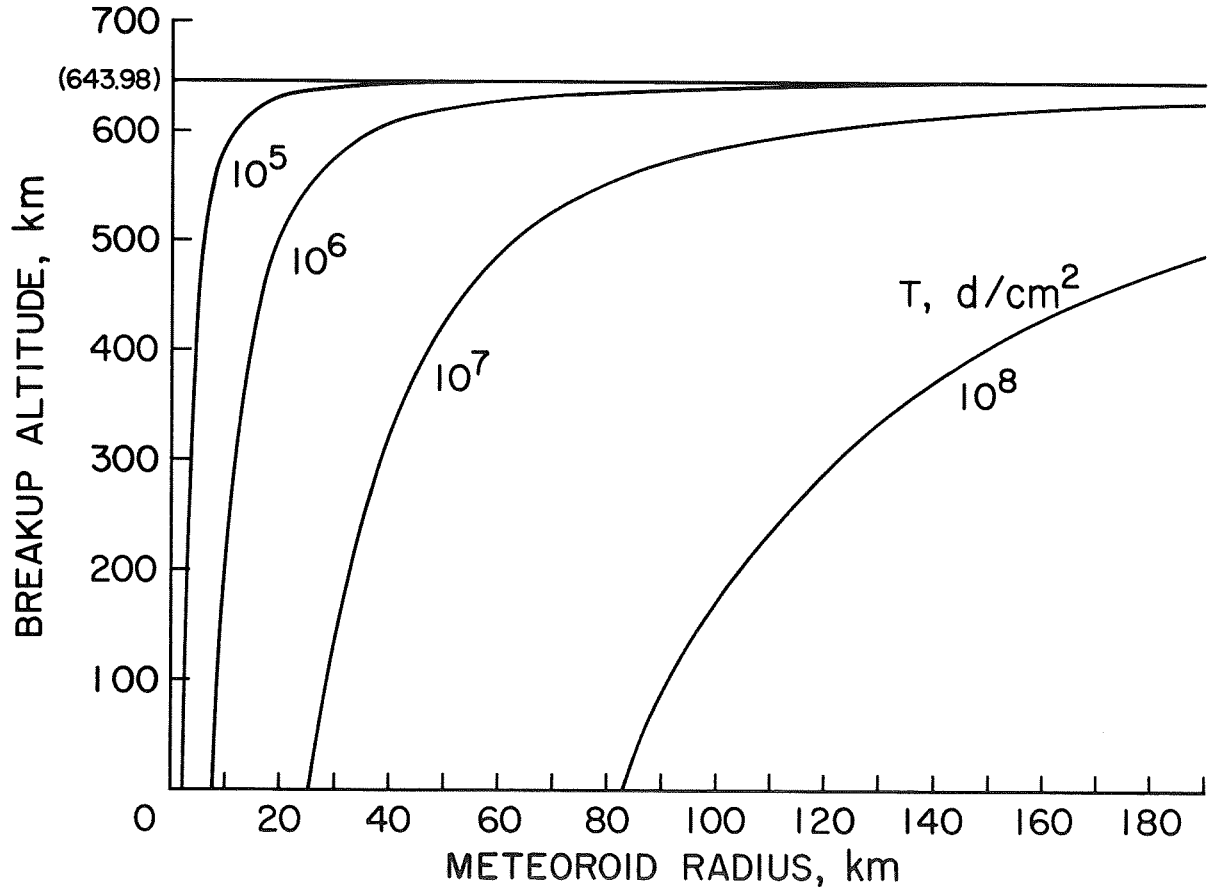
700
(643.98)
600
500
400
300
200
100
0
20
40
60
80
100
120
140
160
180
BREAKUP ALTITUDE, km
METEOROID RADIUS, km
10^5
10^6
10^7
10^8
T, d/cm^2

Figure 8.

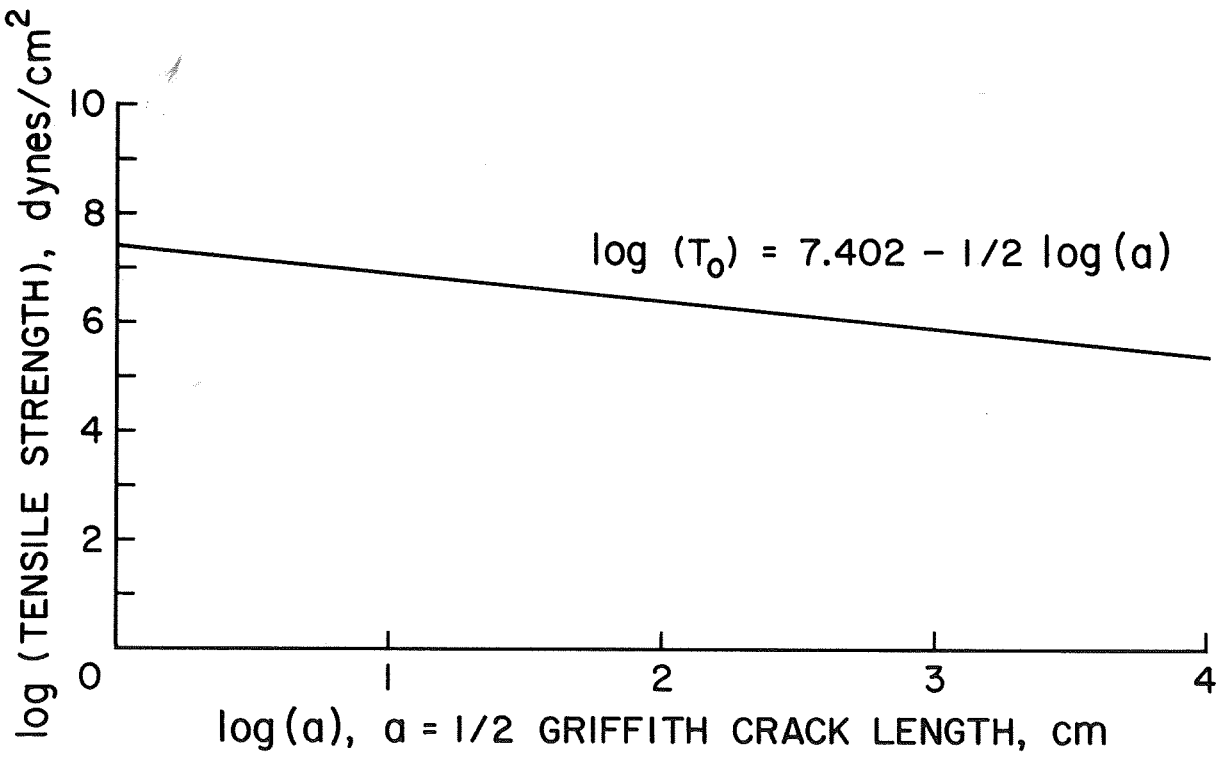
log (TENSILE STRENGTH), dynes/cm^2
10
8
6
4
2
0
log (T_o) = 7.402 − 1/2 log (a)
1
2
3
4
log (a), a = 1/2 GRIFFITH CRACK LENGTH, cm

Figure 9.

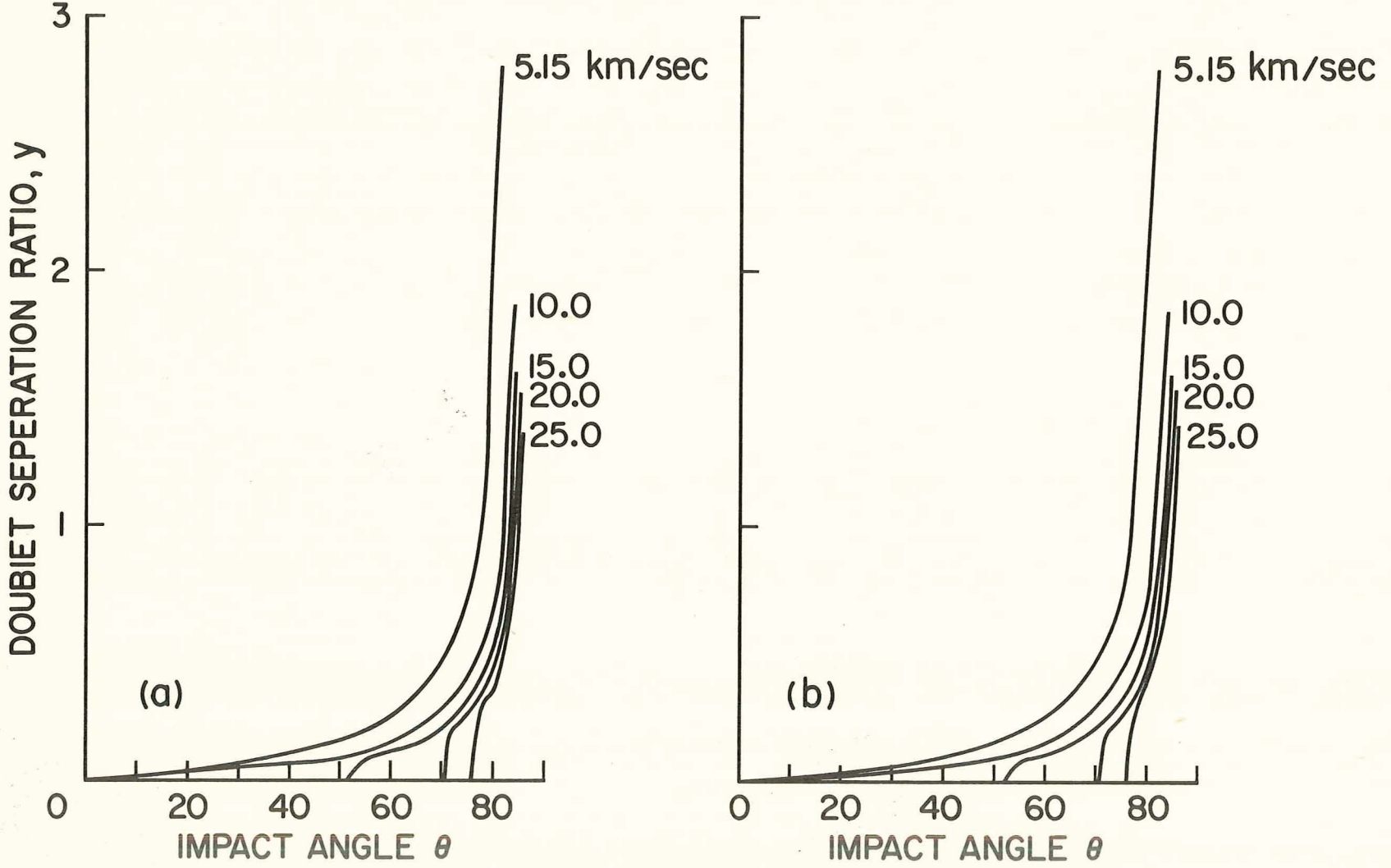
DOUBIET SEPERATION RATIO, y
3
2
1
0
20
40
60
80
IMPACT ANGLE θ
5.15 km/sec
10.0
15.0
20.0
25.0
(a)
(b)

Figure 10.

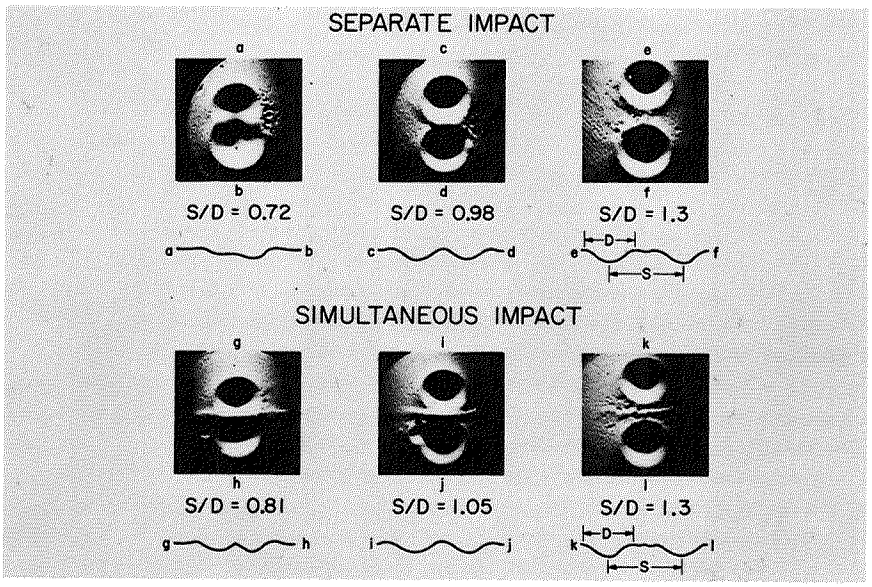
SEPARATE IMPACT
a
b
S/D = 0.72
a
b
c
d
S/D = 0.98
c
d
e
f
S/D = 1.3
D
S
e
f
SIMULTANEOUS IMPACT
g
h
S/D = 0.81
g
h
i
j
S/D = 1.05
i
j
k
l
S/D = 1.3
D
S
k
l

Figure 11.